Dielectric relaxation of ultrathin films of supported polysulfone

Diana Labahn, Renate Mix, and Andreas Schönhals*
Federal Institute for Materials Research and Testing (BAM), Unter den Eichen 87, D-12200 Berlin, Germany
(Received 24 September 2008; published 12 January 2009)

The dynamic glass transition (α relaxation, structural relaxation) of ultrathin polysulfone films prepared between aluminum electrodes is investigated by dielectric relaxation spectroscopy. As a main result, it is found that the glass transition temperature T_g does not depend on the thickness of the polymeric layer down to a thickness of 10 nm. For thicknesses lower than 10 nm, an increase of T_g is observed. A more detailed analysis of the temperature dependence of the relaxation rates reveals that the Vogel temperature increases and the fragility decreases systematically with decreasing film thickness d. Further, the dielectric strength $\Delta\varepsilon$ decreases with decreasing d. This is discussed by the formation of a surface layer of adsorbed polysulfone segments having a reduced molecular mobility with regard to the time scale characteristic of the glassy dynamics of bulk polysulfone. Plotted versus inverse film thickness $\Delta\varepsilon$ decreases linearly with $1/d$ and becomes zero for an extrapolated length scale of 10 nm. From that it is concluded that the thickness of the adsorbed boundary layer is about 5 nm. Contact-angle measurements were carried out to confirm the strong interaction between aluminum and polysulfone. It is also shown that preparation details like annealing conditions strongly influence the glass transition of supported ultrathin films.

DOI: 10.1103/PhysRevE.79.011801 PACS number(s): 82.35.Gh, 77.55.+f

I. INTRODUCTION

Ultrathin polymer films are of considerable interest technologically in a wide range of areas ranging from coatings to organic electronic devices. This is due to reasons that include tunability of the properties, low production costs, and high flexibility. Since the pioneering work of Keddie and Jones [1], the structural and dynamic properties of thin polymer films have been in the focus of scientific discussion [2–5]. A variety of problems have to be understood from a fundamental point of view. This includes, for instance, wetting [6], viscoelastic properties [7], diffusion processes [8], and most importantly the glass transition phenomenon [1,2] because the glass transition temperature T_g is a key property for the application of thin polymer films. Among other methods like ellipsometry [1,9], x-ray and neutron scattering [10–13], Brillouin light scattering [14–16], and fluorescence spectroscopy [17–19], dielectric spectroscopy is a powerful tool to study the molecular dynamics of ultrathin polymer films [5]. Several groups have used extensively that method to investigate the molecular dynamics of different polymers in thin films [20–30]. For a review of the dynamics of polymers in thin films and molecules in confinement in general, see Ref. [31].

From the rich numbers of experimental investigations, one can conclude that the dependence of the glass transition temperature T_g on the film thickness of ultrathin supported films is controversially discussed in the literature. T_g seems to be controlled by several effects. The both most important are the thickness of the polymer film (confinement effect) and the interaction of polymer segments with the supporting substrates. In addition to that, the preparation (annealing) and the used experimental method may also play a role. Just to mention a few examples, in their pioneering work Keddie *et al.* [1] found a decrease of the glass transition temperature with decreasing film thickness for polystyrene (PS) almost independent from the nature of the substrate (gold, silicon oxide). In contradiction to that, dielectric spectroscopy gives that the T_g of PS films prepared on an aluminum support is almost independent of the layer thickness down to a few nm [24,28]. Poly(methyl methacrylate) (PMMA) spin coated on gold surfaces shows a decreases of T_g with decreasing layer thickness where an increase of T_g is found for a silicon oxide substrate [1]. A detailed study of the role of the polymer-surface interaction for glassy dynamics of thin supported polymer films is given in Ref. [11]. There it is concluded that for lower values of the polymer-surface energy γ_{SP} than a critical one γ_{sp}^{*} the glass transition temperature decreases where for $\gamma_{SP} > \gamma_{sp}^{*}$ an increase of T_g is observed. In Ref. [12] it is concluded that the polymer-surface energy γ_{SP} alone is an insufficient parameter to describe the glass transition in ultrathin polymer layers. Also the density of the segments close to the surface should be considered.

One can further argue that the free surface of the polymer film (polymer-air interface) characteristic of ellipsometry and fluorescence measurements is important for the strong T_g depression with decreasing film thickness found by these methods where dielectric measurements, where the film is prepared between aluminum electrodes, often show a constant value of T_g down to a few nanometers. Recently, a new method for dielectric measurements was developed where one side of the film is also free [32]. Also, these measurements show no T_g shift with decreasing film thickness for a variety of polymers. Moreover, specific heat-capacity spectroscopy using a chip calorimeter where the sample has also a free surface gives similar results [29,32]

To be complete in addition to the mentioned effects also the formation of a chemical bond between the surface and the polymer can play a role. So for poly(ethylene terephthalate) (PET) spin coated on aluminum the formation of bonds between the carbonyl group (—C═O) of the polymer and

*Corresponding author: Andreas.Schoenhals@bam.de

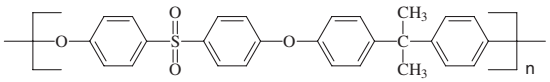

FIG. 1. Chemical structure of polysulfone.

the Al of the surface was reported for both PET/Al and PET/AlO_x interfaces [33–35]. For the case of polymers grafted on a surface, a strong increase of T_g was reported even for rather large layer thicknesses [36].

In this contribution dielectric relaxation spectroscopy is employed to investigate the molecular dynamics of ultrathin polysulfone (PSU) films were PSU is spin coated on aluminum. The obtained results are compared with data obtained for polysulfone spin coated on a quartz slide with a native oxide surface layer investigated by fluorescence spectroscopy [19] and for PSU on the native oxide surface of a silicon wafer studied by ellipsometry [9]

II. EXPERIMENT

Polysulfone having a molecular weight of M_w =45 000 g/mol and a polydispersity index of 1.6 was purchased from Sigma-Aldrich. Its chemical structure is given in Fig. 1. Size exclusion chromatography proves that there are no significant low-molecular-weight contributions or monomeric components. The glass transition temperature T_g of the bulk material is estimated to 457 K (DSC, 10 K/min, second heating run). Polysulfone is an amorphous polymer which does not crystallize.

The ultrathin films were prepared between two aluminum electrodes. Glass slides of 2.5 cm×2.5 cm×1 mm were used as substrate. The slides were cleaned in a first step in an ultrasound alkaline bath at 333 K for 15 min followed by a second ultrasound bath with ultrahigh purified water (Millipore, resistivity >18 MΩ/cm). Then the glass plates were first rinsed in acetone and then in chloroform (both solvents Uvasol quality). After that, the substrates were dried in a nitrogen flow. An aluminum electrode (width 2 mm, height ca. 60 nm) was deposited onto the glass substrate by thermal evaporation in an ultrahigh vacuum (10^{-6} mbar). After the evaporation of this first electrode, the plates were again rinsed in acetone and chloroform. Subsequently, a thin polymer film was spin coated from a filtered chloroform solution at 3000 rpm. The film thickness was adjusted by changing the concentration of the polymer in the solution. After spin coating, the sample was annealed or equilibrated at a temperature well above the bulk glass transition ($T_{ann}=T_{g,bulk}$ +35 K) in an oil-free vacuum (10^{-3} mbar) for 24 h. The quality of the film was checked by imagine the topography by atomic force microscopy (AFM) measurements (tapping mode). Down to 10 nm, homogeneous films with a low roughness are obtained by this procedure. No dewetting was detected.

The preparation was finalized by the evaporation of the counterelectrode on the top of the polymer film. In general, evaporation of metals can damage the polymer surface as discussed in Ref. [37]. To minimize the diffusion of metal atoms into the film and to avoid damages of the polymer, a so-called flash evaporation was applied. This means the evaporation time was kept as short as possible (<2 s). It is known that under these conditions a sharp and smooth metal/polymer interface is obtained [38]. Also, pinholes were not observed because pinholes would preclude the dielectric measurements. Prior to the measurement, the sample was annealed again at ($T_{ann}=T_{g,bulk}+35$ K, in an oil-free vacuum 10^{-3} mbar, 24 h) to relax the internal stresses introduced by the evaporation of the second electrode. It should be noted here that due to the preparation condition, a thin aluminum oxide layer (1–2 nm) might be formed at the bottom electrode. This layer can influence the dielectric behavior, but equivalent circuit models can be applied to estimate its influence.

To study the influence of the annealing temperature on the molecular dynamics of thin PSU films, samples with a thickness of 20 nm were annealed at different temperatures from close to $T_{g,bulk}$ up to $T_{ann}=T_{g,bulk}+35$ K.

The corresponding bulk sample was obtained by casting from a chloroform solution on a polished glass substrate. To control the initial evaporation of the solvent from that thick film, the glass plate was placed in a closed chamber. To remove the residual solvent, the bulk sample was annealed using the same conditions than for the ultrathin films ($T_{ann}=T_{g,bulk}+35$ K in an oil-free vacuum (10^{-3} mbar) for 24 h).

A high-resolution ALPHA analyzer (Novocontrol) is used to measure the complex dielectric function $\varepsilon^*(f)=\varepsilon'(f)-i\varepsilon''(f)$ (f, frequency; ε' and ε'', real and imaginary parts of the complex dielectric function, $i=\sqrt{-1}$) in the frequency range from 10^{-1} to 10^7 Hz. The temperature was controlled by a Quatro Novocontrol cryosystem with a temperature stability better than 0.1 K. For more details, see Ref. [39]. It is worth mentioning that during the whole measurement the sample was kept in a pure nitrogen atmosphere.

The film thickness d was determined by measuring the real part of the sample capacitance C' in a spectral region not affected by dielectric dispersions ($T=298$ K, $f=1$ kHz). It holds

$$d=\frac{\varepsilon_0\varepsilon' A}{C'} \tag{1}$$

with ε_0 the permittivity of free space and A the electrode area (4 mm^2). ε' is the permittivity of the bulk sample estimated to 3.7 at $T=298$ K for 1 kHz. For a few samples this procedure was checked by the absolute thickness measurements by AFM.

III. RESULTS AND DISCUSSION

Bulk polysulfone shows at least two relaxation processes indicated by peaks in the dielectric loss ε'' (see Fig. 2). The β relaxation at low temperatures is assigned to localized fluctuations. At higher temperatures than the β process, the α relaxation (dynamic glass transition) takes place. This relaxation process is related to cooperative segmental fluctuations of PSU. There might be some indications that in the temperature range between the β and α processes are further pro-

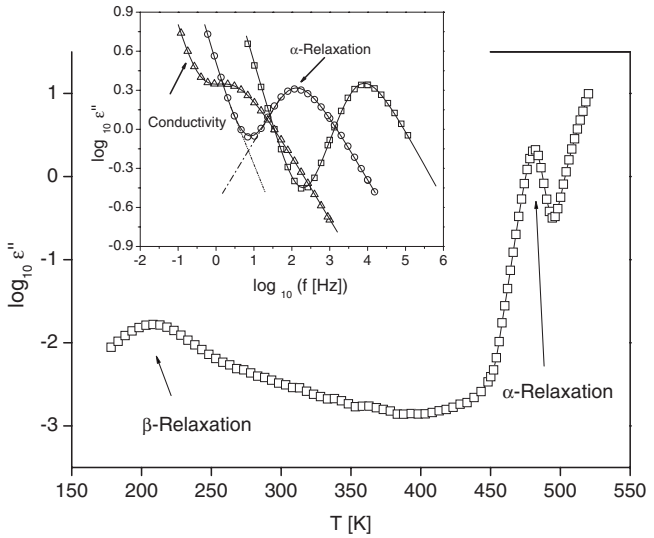

FIG. 2. Dielectric loss vs temperature for pure PSU at a frequency of 1 kHz. The line is a guide for the eyes. The inset gives the dielectric loss versus frequency for three different temperatures above T_g: △, 465 K; ○, 476 K; □, 488 K. The solid lines are fits of the HN function to the data including a conductivity contribution. The dashed line gives the contribution for the α relaxation for T =476 K.

cesses, but the dielectric loss is low and no pronounced peak can be observed. Additional investigations are necessary to clear up this.

The model function of Havriliak and Negami (HN) [40] is used to analyze the dielectric measurements quantitatively. It reads

$$\varepsilon^*_{\mathrm{HN}}(\omega) - \varepsilon_\infty = \frac{\Delta\varepsilon}{[1 + (i\omega/\omega_0)^\beta]^\gamma}. \tag{2}$$

ω_0 is a characteristic frequency related to the frequency of maximal loss f_p (relaxation rate). The explicit relationship between both is discussed in detail in Ref. [41]. ε_∞ describes the value of the real part ε' for $f \gg f_0$. β and γ are fractional parameters $(0<\beta\leqslant 1$ and $0<\beta\gamma\leqslant 1)$ characterizing the shape of the relaxation time spectra. $\Delta\varepsilon$ denotes the dielectric strength. From the fit of the HN function to the data, the relaxation rate f_p and the dielectric strength are determined and further discussed. Conduction effects are treated in the usual way by adding a contribution $\varepsilon''_{\mathrm{cond}}=\sigma_0/[\omega^s\varepsilon_0]$ to the dielectric loss where σ_0 is related to the specific dc conductivity of the sample. The parameter $s(0<s\leqslant 1)$ describes for $s=1$ Ohmic and for $s<1$ non-Ohmic effects in the conductivity. For details, see Ref [41]. Some examples of fitting the HN equation to the α relaxation of bulk PSU are given in the inset of Fig. 2.

Figure 3 gives the temperature dependence of the relaxation rates for the α relaxation and in the inset of Fig. 3 for the β process of bulk PSU. As is known for glassy dynamics, $f_{p,\alpha}(T)$ is curved versus $1/T$, which can be described by the Vogel-Fulcher-Tammann (VFT) equation [42]

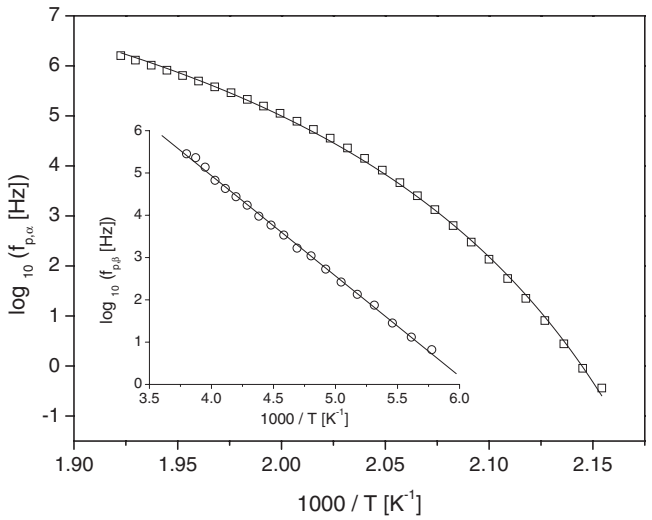

FIG. 3. Relaxation rate $f_{p,\alpha}$ vs $1/T$ for the α relaxation of bulk polysulfone. The line is a fit of the VFT equation to the data. The inset gives $f_{p,\beta}$ vs $1/T$ for the β relaxation of bulk PSU. The line is a fit of the Arrhenius equation to the data.

$$\log_{10} f_p = \log_{10} f_\infty - \frac{A}{T - T_0} = \log_{10} f_\infty - \frac{\ln(10) D T_0}{T - T_0} \tag{3}$$

($\log f_\infty$ and A are constants, and T_0 is the so-called Vogel temperature). The degree of deviation from an Arrhenius-type temperature dependence provides a useful classification of glass formers [43,44]. Materials are called "fragile" if their $f_p(T)$ dependence deviates strongly from an Arrhenius-type behavior and "strong" if $f_p(T)$ is close to the latter. Despite other possibilities, the parameter $D=\frac{A}{T_0 \ln(10)}$ in Eq. (3) can be used as a quantitative measure of the "fragility" [43,44]. All estimated parameters are given in Table I. For the β relaxation the temperature dependence of the relaxation rate obeys the Arrhenius equation with an activation energy of 45.4 kJ/mol and a prefactor $\log(f_\infty\,[\mathrm{Hz}])=14.4$.

For the samples in thin-film geometry, an additional effect has to be considered in the data analysis because for the thin-film capacitors the resistance R of the Al electrodes can-

TABLE I. Estimated VFT parameters and dielectric glass transition temperatures T_g^{diel}.

Thickness [nm]	$\log_{10}(f_\infty[\mathrm{Hz}])$	A [K]	T_0 [K]	T_g^{diel} [K] $f=10$ Hz	T_g^{diel} [K] $f=0.1$ Hz
Bulk	10.8	429.3	426.7	470.5	463.3
220	12.15	613.6	418.4	473.4	465.1
138	11.5	523.3	421.7	471.5	463.5
107	9.4	306.7	435.7	472.2	465.2
48	9.3	270.6	439.1	471.7	465.3
23	8.4	191.2	444.5	470.3	464.8
20	8.2	168.0	447.8	471.1	466.0
14	8.0	190.7	445.6	472.8	466.8
9.6	8.0	60.0	464.5	482.5	471.6

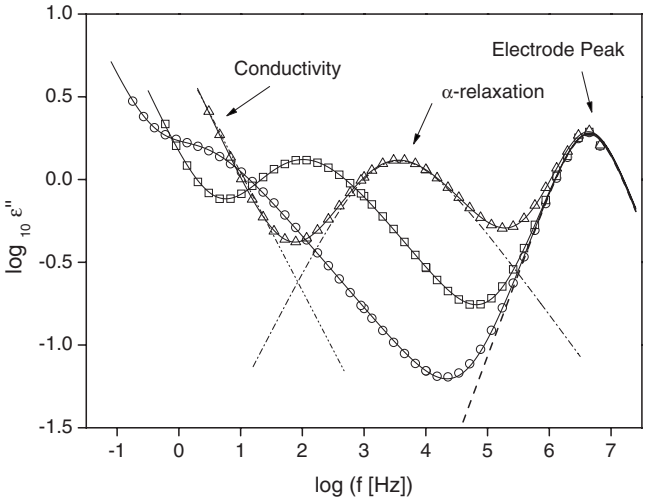

FIG. 4. Dielectric loss vs frequency of a polysulfone film with a thickness of 48 nm for different temperatures: ○, 469 K; □, 477 K; △, 487 K. The solid lines are fits of Eq. (4) to the data. The dashed lines are the contributions of the conductivity (dash–double-dotted line), the α relaxation (dash-dotted line), and the resonance peak (dashed line) for T=477 K.

not be neglected. This resistance leads to an artificial loss peak (electrode peak) on the high-frequency side of the spectra with a time constant $\tau_{\mathrm{res}}=R^*C'$ (C' is the sample capacity). This means with decreasing film thickness C' increases and the electrode peak shifts to lower frequencies. Because its peak shape in the frequency domain obeys a Debye-type equation, it can be subtracted using the following fit function:

$$\varepsilon^*_{\mathrm{fit}} = \varepsilon^*_{\mathrm{HN}}(\omega) - i\frac{\sigma}{\omega^s \varepsilon_0} + \frac{\Delta\varepsilon_{\mathrm{res}}}{1 + i\omega\tau_{\mathrm{res}}}. \tag{4}$$

Figure 4 gives an example for the analysis of the dielectric spectra of a thin polysulfone film with a thickness of 48 nm for different temperatures. As expected, the frequency position of the artificial loss peak is independent of temperature.

In Fig. 5 the relaxation rate $f_{p,\alpha}$ is plotted versus $1/T$ for different film thicknesses. Besides for the lowest layer thickness all other data are more or less independent of the thickness of the film. At first glance this points to a weak influence of the thickness of the PSU layer on its glass transition temperature T_g. As a measure for T_g, a dielectric glass transition temperature T_g^{diel} is estimated by $T_g^{\mathrm{diel}}=T(f_{p,\alpha}=C\ [\mathrm{Hz}])$. These estimations were done for two values of the frequency C, 10 Hz and 0.1 Hz. For both values of C, T_g^{diel} is plotted versus film thickness d in Fig. 6 and displays a similar behavior. As is already concluded from the raw data down to a film thickness of 10 nm, the glass transition temperature is independent of d. For thicknesses lower than 10 nm, an increase of T_g^{diel} with decreasing d is observed.

To analyze the temperature dependence of the relaxation rate in more detail, a derivative method is used [45]. This method is sensitive to the functional form of $f_p(T)$ irrespective of the prefactor f_∞. For a dependence according to the VFT equation, one gets

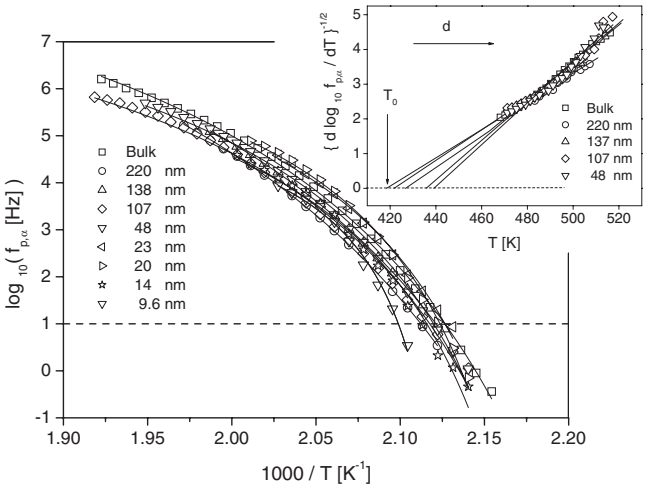

FIG. 5. Relaxation rate $f_{p,\alpha}$ vs $1/T$ for the α relaxation of polysulfone films for the labeled film thicknesses. The lines are fits of the VFT equation to the data as described in the text. The dashed line indicates one frequency of 10 Hz used to estimate the dielectric glass transition temperature T_g^{diel}. The inset gives $(\frac{d\log_{10} f_{p,\alpha}}{dT})^{-1/2}$ versus temperatures for the labeled film thicknesses. Lines are linear regressions to the data.

$$\left[\frac{d\log_{10} f_p}{dT}\right]^{-1/2} = A^{-1/2}(T - T_0). \tag{5}$$

In a plot $[d\log_{10} f_p/dT]^{-1/2}$ versus T a VFT behavior shows up as a straight line (see inset in Fig. 5). First, it is concluded that for all thicknesses the relaxation rates follow the VFT temperature dependence. All experimental data can be well described by straight lines. To estimate the parameters of the VFT equation and the fragility D for a quantitative comparison the following procedure was applied. T_0 and the A parameter were taken from the derivative technique by linear regression. The prefactors were obtained by a fit of the VFT

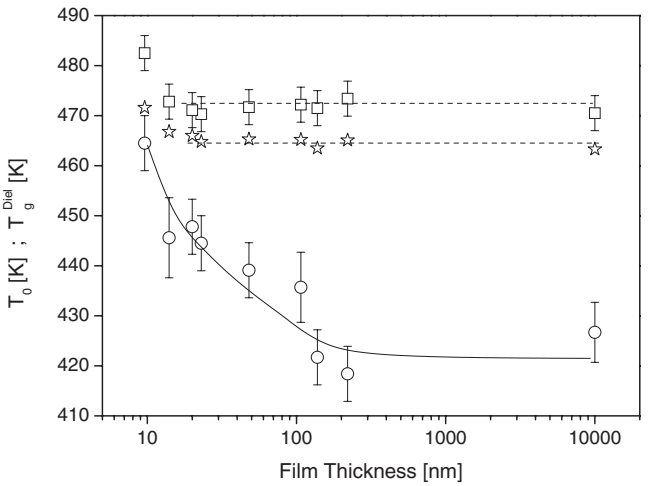

FIG. 6. Dielectric glass transition temperature T_g^{diel} (□, 10 Hz; ☆, 0.1 Hz) and Vogel temperature T_0 (○) vs thickness d of the polysulfone film. Lines are guides for the eyes. Typical error bars are given for T_g^{diel}. The error bar for T_0 results from the linear regression.

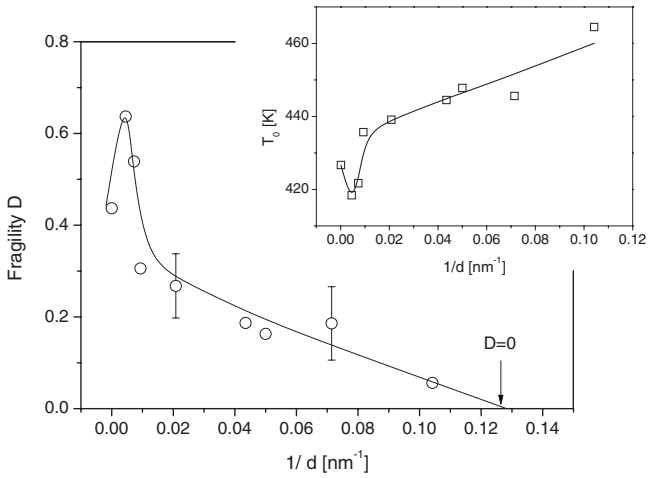

FIG. 7. Fragility parameter D vs inverse film thickness. The line is a guide for the eyes. Typical error bars are given. The inset gives T_0 vs inverse film thickness. The line is a guide for the eyes.

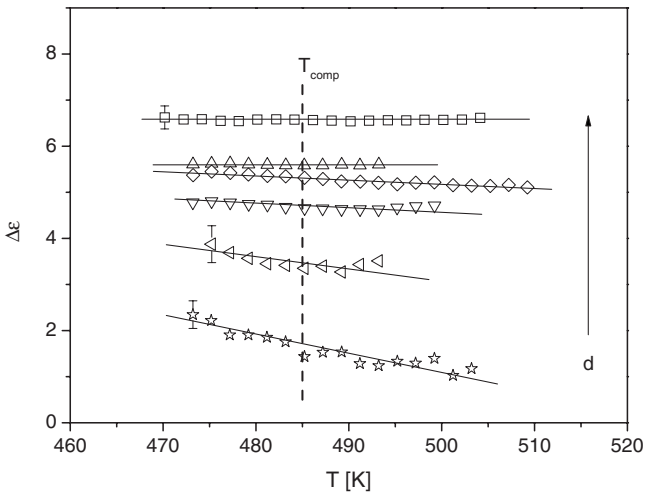

FIG. 8. $\Delta\varepsilon$ vs temperature for different film thicknesses: □, bulk; △, 138 nm; ◇, 107 nm; ▽, 48 nm; ◁, 23 nm; ☆, 14 nm. Some typical error bars are given. Lines are linear regression to the data.

equation to the relaxation rates keeping T_0 and A fixed. All parameters are collected in Table I.

The derivative technique gives as a second result that the Vogel temperature T_0 is influenced by the confinement. With decreasing film thickness, the Vogel temperature increases systematically (see inset in Figs. 5 and 6). This was also found for a few other systems [14,25,26,46] and will be discussed later.

From the estimated VFT parameters, the fragility D is calculated and plotted versus $1/d$ in Fig. 7. With decreasing layer thickness, D decreases and becomes zero at an extrapolated length scale of around 8 nm. This points to a dramatic change in the mechanism of the underlying molecular motions with decreasing film thickness. Why the fragility of the bulk sample is lower than for a 220-nm-thick PSU film is not clear and needs further investigation.

From the fit of the HN function to the data in addition to the relaxation rate also the dielectric strength $\Delta\varepsilon$ is obtained. Its temperature dependence is plotted in Fig. 8 for several layer thicknesses.

With decreasing thickness, $\Delta\varepsilon$ decreases strongly. To discuss this quantitatively $\Delta\varepsilon$ is taken at a temperature of 485 K and plotted versus inverse layer thickness in Fig. 9. The inset of this figure gives $\Delta\varepsilon$ versus d. As already concluded from Fig. 8, $\Delta\varepsilon$ decreases strongly, but follows a linear dependence when plotted versus inverse layer thickness. This is also observed for other polymers [22,26,30]

The Debye theory of dielectric relaxation generalized by Kirkwood and Fröhlich [47] predicts for the temperature dependence of the dielectric relaxation strength

$$\Delta\varepsilon = \frac{1}{3\varepsilon_0} g \frac{\mu^2}{k_B T} \frac{N}{V}, \tag{6}$$

where μ is the mean dipole moment of the process under consideration and N/V is the number density of dipoles involved. g is the so-called Kirkwood-Fröhlich correlation factor, which describes static correlation between the dipoles. The Onsager factor is omitted for the sake of simplicity. It is most natural to assume that the dipole moment does not depend on the thickness of the polymer film. Assuming further that also the correlation factor depends only weakly on the film dimension, it is concluded that the strong decrease of $\Delta\varepsilon$ is due to a strong reduction of the number density of fluctuating dipoles with decreasing film thickness. This can be explained in terms of a multilayer model. Due to the high interfacial energy between PSU and AlO_x (see below), the segments very close to the electrodes interact strongly with the Al substrate. Because of the interaction between the segments, this surface interaction influences the sample properties of a larger area. Therefore these segments have with regard to the time scale of the dynamic glass transition of bulk PSU a strongly reduced mobility. The extension of this reduced mobility layer depends on the substrate polymer interaction and the flexibility of the macromolecule. Samples

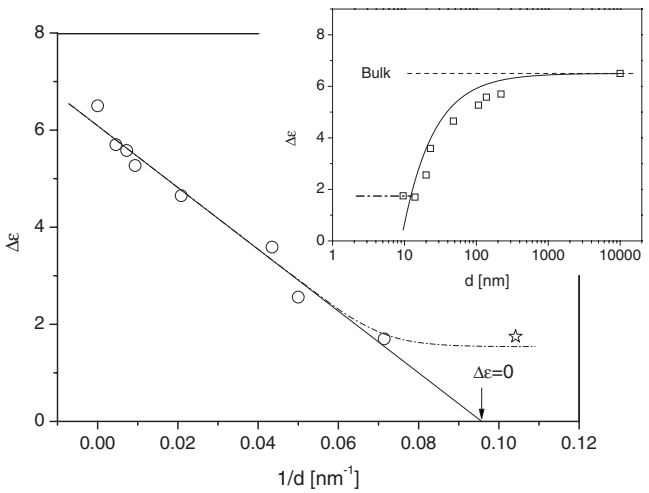

FIG. 9. $\Delta\varepsilon$ vs inverse film thickness for T_{com}=485 K. The dashed-dotted line is a guide for the eyes. The solid line is a linear regression to the data except the point for the lowest layer thickness (☆). The inset gives $\Delta\varepsilon$ vs d. Lines are guides for the eyes.

with less flexible chains like PSU are expected to have a thicker reduced mobility layer.

Except the point for the lowest layer thickness, $\Delta\varepsilon$ versus $1/d$ can be well described by a linear relationship. The extrapolation to $\Delta\varepsilon=0$ gives a length scale of ca. 10 nm, which gives 5 nm as an estimate for the thickness of the reduced mobility layer. This value is in agreement with the length scale where also the fragility parameter becomes zero discussed above (ca. 8 nm), which will give a thickness of 4 nm for this layer. In conclusion, in a simplified model the structure of polysulfone films on the aluminum support has to be considered at least as a two-layer system consisting of a surface layer with a reduced mobility and a layer in the middle of the film which behaves bulk like [25,26]. To be more realistic, a mobility gradient has to be assumed.

The point for the lowest film thickness was excluded from the linear fit shown in Fig. 9. The corresponding film thickness is below 10 nm. Therefore this value was attributed to the surface layer having a reduced mobility and a higher glass transition temperature. This is in accordance with the result that for the lowest layer thickness (9.6 nm) the glass transition temperature is increased by more than 10 K compared to the bulk value. It would be interesting to measures samples with thickness below 9.6 nm to see whether the dielectric strength actually becomes independent of the film thickness at such length scales. Unfortunately, no stable films with lower thicknesses can be prepared by the used experimental method. To be complete one has to mention that the complex dielectric function for the discussed simple two-phase model (bulklike layer, reduced mobility layer) is not additive. Therefore the surface layer with a reduced molecular mobility can have a complicated influence on the measured total dielectric response [48]. This is also discussed in detail in Ref. [26]. Model calculations show [26] that the decrease of the dielectric strength is in full agreement with the existence of an adsorbed layer with a reduced mobility. In addition to that surface layer, the thin oxide layer on the aluminum electrodes can cause a further reduction of the dielectric strength as discussed in Ref. [48]. A quantitative discussion requires some assumptions like a model for the structure. The justification of these assumptions and the values of the input parameters are arguable.

Finally, the thickness of the Vogel temperature can be discussed in the same way. Concerning the experimental results, the polysulfone films has to be considered as a two-layer system as discussed above. With decreasing film thickness the ratio between the amount of the surface layer and that of the bulklike layer increases. One has to keep in mind that dielectric spectroscopy senses the response of the whole film. Therefore the estimated Vogel temperature should be considered as a mean value averaging over the mobility gradient inside the film due to interfacial interactions as also discussed in Ref. [49]. With decreasing film thickness the contribution of the surface layer increases. Figure 7 shows that both the fragility and the Vogel temperature T_0 do not scale linearly with the inverse film thickness. Similar results are also found in Refs. [25,26], which indicate that dielectric spectroscopy does not weight the layer contributions regarding their volume percentage. This points again to the fact that a gradient of molecular mobility instead of a simple two-layer model has to considered.

TABLE II. Contact-angle values of the test liquids with polysulfone. The values for aluminum oxide are taken from Ref. [26].

	Diodomethan	Ethylene glycol	Water	Glycerol
PSU	37.0 ± 3.4	64.9 ± 0.6	103.9 ± 0.4	
AlO_x	63.6 ± 0.1		79.0 ± 0.7	79.0 ± 2

TABLE III. Total surface energy γ^{total} and its dispersive γ^{LW} and polar components γ^P for the test liquids according to the data given in Ref. [51].

	Diodomethan	Ethylene glycol	Water	Glycerol
γ^{total} [mN/m]	50.8	48.0	72.80	64.0
γ^{LW} [mN/m]	48.5	29.0	26.00	34.0
γ^+ [mN/m]	0	2.60	34.2	5.3
γ^- [mN/m]	0	34.8	19.0	42.5

To estimate the interfacial energy between aluminum oxide AlO_x and polysulfone contact angle, measurements were carried out. Diodomethan, ethylene glycol, and water have been used as test liquids. The measurements were carried out using the automated contact-angle system G2 (Krüss) by the Sessile drop method. To estimate the values for AlO_x, the contact angles are taken from Ref. [26]. The angle values are given in Table II. The contact-angle values were used as input to calculate the interfacial energy γ_{SP} in the frame of the Fowkes–van Oss–Chaudry–Good (FOCG) model [11,50]. In this model the surface tension is given by $\gamma^{\text{total}}=\gamma^{\text{LW}}+\gamma^P=\gamma^{\text{LW}}+2\sqrt{\gamma^+\gamma^-}$, where γ^{LW} is the dispersive and γ^P the polar component. The equation of Young and Dupré [50] was applied to estimated γ^{LW}, γ^+, and γ^-. The corresponding values for the test liquids used for that analysis are taken from Ref. [51] and listed in Table III. The values obtained for both aluminum and polysulfone are displayed in Table IV. The polar component is further expressed by the electron-acceptor γ^+ and electron-donor components γ^- [50,51]. The Good-Girifalco-Fowkes [52] combining rule was applied to estimate γ_{SP} between PET and AlO_x:

$$\gamma_{\text{SP}}=(\sqrt{\gamma_S^{\text{LW}}}-\sqrt{\gamma_P^{\text{LW}}})^2+2[(\gamma_S^+\gamma_S^-)^{1/2}+(\gamma_P^+\gamma_P^-)^{1/2}-(\gamma_S^+\gamma_P^-)^{1/2}-(\gamma_S^-\gamma_P^+)^{1/2}]. \quad (7)$$

S and P refer to the substrate and polymer. According to Eq. (7), the dispersive part of the AlO_x/PSU is 1.59 mN/m and the polar one is 3.8 mN/m, leading to a total energy of

TABLE IV. Total surface energy γ^{total} and its dispersive γ^{LW} and polar components γ^P for polysulfone and aluminum oxide.

	γ^{total} [mN/m]	γ^{LW} [mN/m]	γ^+ [mN/m]	γ^- [mN/m]
PSU	41.1	41.1	≈0	0.2
AlO_x	30.4	26.5	0.5	7.7

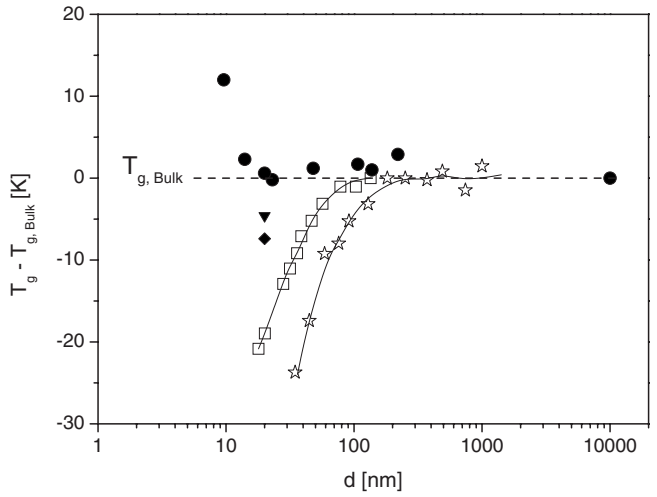

FIG. 10. Dependence of the glass transition temperatures vs film thickness for thin polysulfone films: ●, dielectric data (C=10 Hz), this publication. The error bars are the same than in Fig. 6, □, data measured by Kim *et al.* [9]: ☆, data published by Torkelson *et al.* [19]. The lines are guides for the eyes. ▼, dielectric data measured for a 20-nm-thick film annealed at T=473 K; ◆, dielectric data measured for a 20-nm-thick film annealed at T=463 K.

5.45 mN/m. In comparison to the values given in Ref. [11], the value found here is essential higher and in a region which correspond to a strong increase of T_g ($\gamma_{SP}^{*} \approx 2$ mN/m for different couples of substrates and polymers [11]). To be complete the real interfacial energy could be higher than the calculated γ_{SP} due to the formation of chemical bonds or specific interaction between Al and PSU, for instance, via the sulfonate group. The discussion of this point is out of the scope of this paper and is currently studied by detailed x-ray photoelectron spectroscopy (XPS) investigations [53].

Torkelson *et al.* [19] investigated the dependence of T_g of polysulfone layers prepared on the surface of a quartz slide by fluorescence spectroscopy. Ellipsometry was employed by Kim *et al.* [9] to study the thickness dependence of the glass transition temperature of thin PSU layers spin coated on the native oxide surface of a silicon wafer. The corresponding T_g values were taken from these publications, and the difference to the bulk T_g value is plotted versus the layer thickness in Fig. 10 and compared to the dielectric data discussed here. For both systems a strong decrease of T_g with decreasing layer thickness is observed where the dielectric data show almost no thickness dependence as discussed. The reason for this diverging behavior might be the different interactions of the polysulfone segments with the different substrates and/or different preparation conditions. Another point to discuss is that the samples investigated here are capped between two aluminum electrodes. The samples studied by Kim *et al.* and Torkelson *et al.* had one polymer/air interface (free surface). It is often argued that this free surface is responsible for the significant reduction in the glass transition temperature [29]. This might be one further reason for the differences in these data sets. But, however, it should be also mentioned that recent dielectric and thermal measurements for samples with one free surface did not report any significant T_g reduction [32]. To shine some light on the influence of the preparation conditions, experiments are carried for a 20-nm-thick polysulfone film annealed at different temperatures above the bulk glass transition temperature of PSU. The results are included in Fig. 10. With decreasing annealing temperature the estimated T_g decreases and becomes comparable with the data reported in Refs. [9,19]. This decrease of T_g should be not attributed to residual solvent left inside the sample because the layer thickness is small. It is likely due to a nonequilibrium state of polysulfone segments (compared to bulk PSU) introduced by the preparation of the film. By spin coating the polymer, chains are transferred from the solution to a solid state in a short time. This corresponds first to extremely high cooling rates. Second, for ultrathin films, the surface layer formed by strongly adsorbed segments dominates the properties of the whole film. Because this surface layer has an essential lower molecular mobility, the equilibration of it needs a longer time or higher temperatures than for the corresponding bulk. Insufficient equilibration conditions can lead to frustrated structures of the polymer, which can give rise to different properties like T_g. From these experiments one can conclude that the preparation conditions may have an essential influence on the properties of ultrathin polymer films.

IV. CONCLUSION

Ultrathin films of polysulfone were prepared from a chloroform solution by spincoating between aluminum layers serving as electrodes for the dielectric measurements. The film thickness was adjusted by varying the concentration of the polymer in the solution from microns down to values below 10 nm. The so prepared samples were studied by dielectric spectroscopy in the frequency range from 10^{-1} to 10^{7} Hz.

The bulk PSU sample shows two different relaxation processes characteristic of amorphous polymers: an activated β process at low temperatures and α relaxation (dynamic glass transition) for temperatures above T_g.

For the thin films a dielectric glass transition temperature T_g^{diel} was calculated from the temperature dependence of the relaxation rates $f_{p,\alpha}$ by $T_g^{\mathrm{diel}}=T(f_{p,\alpha}=C\ [\mathrm{Hz}])$ as a measure for T_g. For the selected two frequencies C (10 and 01 Hz), T_g^{diel} does not depend on the thickness of the film down to thicknesses of 10 nm. For lower thicknesses than 10 nm, an increase of T_g was found. This behavior is in pronounced contrast to the behavior reported by Torkelson *et al.* [19] for thin PSU layers on a native quartz surface investigated by fluorescence spectroscopy and the results found by Kim *et al.* [9] for polysulfone spin coated on the native oxide surface of a silicon wafer. Both groups found a strong depression of T_g with decreasing layer thickness. The reason for this discrepancy might be the different interactions of the polysulfone segments with the different substrates and/or different preparation conditions. To explore the latter point experiments are carried out for a 20-nm-thick PSU annealed at different temperatures above the glass transition temperature of bulk polysulfone. With decreasing annealing temperature, T_g^{diel} decreases and comes close to the values reported in Refs. [9,19]. This decrease of T_g^{diel} is probably not due to

traces of solvent left in the film because its thickness is small. More likely is to assume that spin coating introduces a nonequilibrium state of the macromolecules which needs longer times or higher temperatures to be relaxed. This proves that the preparation condition of ultrathin polymeric films can have an essential influence on its properties.

To explore the interaction of the PSU segments with the aluminum oxide surface the dielectric relaxation strength $\Delta\varepsilon$ was estimated from the measurements. It is proportional to the dipole density taking part in the α relaxation. With decreasing film thickness a pronounced decrease of $\Delta\varepsilon$ was observed which is attributed to the formation of a surface layer of polysulfone segments which interacts strongly with the aluminum surface. Therefore this layer has a reduced molecular mobility compared to bulk PSU. The existence of such a layer was confirmed by contact-angle measurements from which the interfacial energy between aluminum oxide AlO_x and polysulfone is estimated. From the thickness dependence of the dielectric relaxation strength, it was concluded that the thickness of this surface layer is ca. 5 nm.

ACKNOWLEDGMENTS

We are grateful to Dr. A. Serghei (University Leipzig) and Professor Dr. M. Wübbenhorst (University Leuven) for fruitful discussions. Dr. J. Falkenhagen (BAM) is thanked for carrying out the SEC measurements to estimate the molecular weight of PSU. D. Silbernagel and Dr. B. Cappella (BAM) are thanked for their help in characterizing the film thickness by atomic force microscopy. The financial support from BAM (D.L.) is appreciated.

[1] L. J. Keddie and R. A. L. Jones, Faraday Discuss. **98**, 219 (1994); L. J. Keddie, R. A. L. Jones, and R. A. Cory, Europhys. Lett. **27**, 59 (1994).
[2] J. R. Dutscher, K. Dalnoki-Veress, and J. A. Forrest, in *Supramolecular Structure in Confined Geometries*, edited by G. War and S. Manne (American Chemical Society, Washington, D.C., 1999).
[3] J. A. Forrest and R. A. L. Jones, in *Polymer Surfaces: Interfaces and thin films*, edited by A. Karim and S. Kumar (World Scientific, Singapore, 2000).
[4] *Proceedings of the Second International Workshop on Dynamics in Confinement*, edited by B. Frick, M. Koza, and R. Zorn [Eur. Phys. J. E **12** (2003)].
[5] L. Hartmann, K. Fukao, and F. Kremer, in *Broadband Dielectric Spectroscopy*, edited by F. Kremer and A. Schönhals (Springer, Berlin, 2002), p. 433.
[6] P. G. de Gennes, Rev. Mod. Phys. **57**, 827 (1985).
[7] H. W. Hu and S. Granick, Science **258**, 1339 (1992).
[8] X. Zheng, B. B. Sauer, J. G. van Alsten, S. A. Schwarz, M. H. Rafailovich, J. Sokolov, and M. Rubinstein, Phys. Rev. Lett. **74**, 407 (1995).
[9] J. H. Kim, J. Jang, and W.-C. Zin, Langmuir **16**, 4064 (2000).
[10] W. J. Orts, J. H. van Zanten, W. L. Wu, and S. K. Satija, Phys. Rev. Lett. **71**, 867 (1993).
[11] D. S. Fryer, R. D. Peters, E. J. Kim, J. E. Tomaszewski, J. J. de Pablo, P. F. Nealey, C. C. White, and W. L. Wu, Macromolecules **34**, 5627 (2001).
[12] O. K. C. Tsui, T. P. Russell, and C. J. Hawker, Macromolecules **34**, 5535 (2001).
[13] T. Kanaya, T. Miyazaki, H. Watanabe, K. Nishida, H. Yamana, S. Tasaki, and D. B. Bucknall, Polymer **44**, 3769 (2003).
[14] J. A. Forrest, K. Dalnoki-Veress, J. R. Stevens, and J. R. Dutcher, Phys. Rev. Lett. **77**, 2002 (1996).
[15] J. A. Forrest, K. Dalnoki-Veress, and J. R. Dutcher, Phys. Rev. E **56**, 5705 (1997).
[16] K. Dalnoki-Veress, J. A. Forrest, C. Murray, C. Gigault, and J. R. Dutcher, Phys. Rev. E **63**, 031801 (2001).
[17] C. B. Roth, K. L. McNerny, W. F. Jager, and J. M. Torkelson, Macromolecules **40**, 2568 (2007).
[18] C. J. Ellison and J. M. Torkelson, Nature Mater. **2**, 695 (2003).
[19] J. M. Torkelson, R. D. Priestley, P. Rittigstein, M. K. Mundra, L. J. Broadbelt, W. F. Jager, and C. B. Roth, ACS preprints Polymeric Materials: Science and Engineering **97**, 782 (2007).
[20] K. Fukao and Y. Miyamoto, Europhys. Lett. **46**, 649 (1999).
[21] K. Fukao and Y. Miyamoto, Phys. Rev. E **61**, 1743 (2000).
[22] R. D. Priestley, L. J. Broadbelt, J. M. Torkelson, and K. Fukao, Phys. Rev. E **75**, 061806 (2007).
[23] V. Lupascu, S. J. Picken, and M. Wübbenhorst, J. Non-Cryst. Solids **352**, 5594 (2006).
[24] V. Lupascu, H. Huth, C. Schick, and M. Wübbenhorst, Thermochim. Acta **432**, 222 (2005).
[25] S. Napolitano, V. Lupascu, and M. Wübbenhorst, Macromolecules **41**, 1061 (2008).
[26] S. Napolitano, D. Prevesto, M. Lucchesi, P. Pingue, M. D. Acunto, and P. Rolla, Langmuir **23**, 2103 (2007).
[27] A. Serghei and F. Kremer, Phys. Rev. Lett. **91**, 165702 (2003).
[28] A. Serghei, H. Huth, M. Schellenberger, C. Schick, and F. Kremer, Phys. Rev. E **71**, 061801 (2005).
[29] A. Serghei, Y. Mikhailova, H. Huth, C. Schick, K. J. Eichhorn, B. Voit, and F. Kremer, Eur. Phys. J. E **17**, 199 (2005).
[30] A. Serghei, M. Tress, and F. Kremer, Macromolecules **39**, 9385 (2006).
[31] M. Alcoutlabi and G. B. McKenna, J. Phys.: Condens. Matter **17**, R461 (2005).
[32] A. Serghei, H. Huth, C. Schick, and F. Kremer, Macromolecules **41**, 3636 (2008).
[33] R. Cueff, G. Baud, M. Benmalek, J. P. Besse, J. R. Butruille, and M. Jacquet, Surf. Coat. Technol. **80**, 96 (1996).
[34] Q. T. Le, J. J. Pireaux, R. Caudano, P. Leclere, and R. Lazzaroni, J. Adhes. Sci. Technol. **12**, 999 (1998).
[35] L. Sandrin and E. Sacher, Appl. Surf. Sci. **135**, 339 (1998).
[36] R. S. Tate, D. S. Fryer, S. Pasqualini, M. F. Montague, J. J. de Pablo, and P. F. Nealey, J. Chem. Phys. **115**, 9982 (2001).
[37] J. S. Sharp and J. A. Forrest, Phys. Rev. Lett. **91**, 235701 (2003).
[38] Th. Strunskus, V. Zaporojtchenko, K. Behnke, C. von Bechtolsheim, and F. Faupel, Adv. Eng. Mater. **2**, 489 (2000).
[39] F. Kremer and A. Schönhals, in *Broadband Dielectric Mea-*

surement Techniques in Broadband Dielectric Spectroscopy, edited by F. Kremer and A. Schönhals (Springer Verlag, Berlin, 2002), p. 35.

[40] S. Havriliak and S. Negami, Polymer **8**, 161 (1967); J. Polym. Sci., Part C: Polym. Symp. **16**, 99 (1966).

[41] A. Schönhals and F. Kremer, in *Analysis of Dielectric Spectra in Broadband Dielectric Spectroscopy*, edited by F. Kremer and A. Schönhals (Springer Verlag, Berlin, 2002), p. 59.

[42] H. Vogel, Phys. Z. **22**, 645 (1921); G. S. Fulcher, J. Am. Ceram. Soc. **8**, 339 (1925); G. Tammann and W. Hesse, Z. Anorg. Allg. Chem. **156**, 245 (1926).

[43] C. A. Angell, J. Non-Cryst. Solids **13**, 131 (1991).

[44] C. A. Angell, J. Res. Natl. Inst. Stand. Technol. **102**, 171 (1997).

[45] F. Kremer and A. Schönhals, in *The Scaling of the Dynamics of Glasses and Supercooled Liquids Spectra in Broadband Dielectric Spectroscopy*, edited by F. Kremer and A. Schönhals (Springer Verlag, Berlin, 2002), p. 99.

[46] K. Fukao, S. Uno, Y. Miyamoto, A. Hoshino, and H. Miyaji, Phys. Rev. E **64**, 051807 (2001).

[47] A. Schönhals and F. Kremer, in *Theory of Dielectric Relaxation Spectra in Broadband Dielectric Spectroscopy* edited by F. Kremer and A. Schönhals (Springer Verlag, Berlin, 2002), p. 1.

[48] S. Peter, S. Napolitano, H. Meyer, M. Wübbenhorst, and J. Baschnagel, Macromolecules **41**, 7729 (2008).

[49] S. Napolitano and M. Wübbenhorst, J. Phys. Chem. B **111**, 9197 (2007).

[50] C. J. van Oss, M. K. Chaudhury, and R. J. Good, Chem. Rev. (Washington, D.C.) **88**, 927 (1988).

[51] L.-H. Lee, Langmuir **12**, 1681 (1996).

[52] R. J. Good and L. A. Girifalco, J. Phys. Chem. **64**, 561 (1960).

[53] A. Schönhals and R. Mix (unpublished).